RESEARCH ARTICLE

# Palladium-Catalyzed Directed *meta*-Selective C–H Allylation of Arenes: Unactivated Internal Olefins as Allyl Surrogates

Tapas Kumar Achar,[a],† Xinglong Zhang,[b],† Rahul Mondal,[a] Shanavas M. S.,[a] Sabyasachi Maity,[a] Nityananda Pal,[a] Robert S. Paton,*[b] and Debabrata Maiti*[a]

**Abstract:** Palladium(II)-catalyzed *meta*-selective C–H allylation of arenes has been developed utilizing synthetically inert unactivated acyclic internal olefins as allylic surrogates. The strong σ-donating and π-accepting ability of pyrimidine-based directing group facilitates the olefin insertion by overcoming inertness of the typical unactivated internal olefins. Exclusive allyl over styrenyl product selectivity as well as *E*-stereoselectivity were achieved with broad substrate scope, wide functional group tolerance and good to excellent yields. Late-stage functionalisations of pharmaceuticals were demonstrated. Experimental and computational studies shed insights on the mechanism and pointed to key palladacyclic steric control in determining product selectivities.

## Introduction

Transition metal catalyzed C–H bond functionalization has emerged as an indispensable tool in late-stage functionalization of complex pharmaceuticals and agrochemicals.[1] However, achieving site-selective C–H functionalization of aromatic compounds is a fundamental challenge due to the inherently similar electronic and steric properties of the C–H bonds.[2] In order to achieve C–H bond functionalization at a desired position, directing group (DG) assistance has been employed extensively for proximal *ortho*-C–H bond activation,[3] whereas distal *meta*- and *para*-C–H bond activations are relatively underexplored.[4] In recent years, remarkable efforts have been expended to establish straightforward *meta*-selective C–H functionalization method.[5] Over the past years, our group has focused on these developments in terms of designing new directing groups, introducing new functionalities and understanding the reaction mechanisms.[6] The use of nitrile DG for *meta*-C–H functionalization confines the method to the introduction of less reactive coupling partners due to the week coordination and side-on binding of the nitrile.[5e] In 2017, we introduced a stronger coordinating pyrimidine-based DG which was more efficacious than nitrile DG for the introduction of different functionalities.[6a, 7]

[a] Dr. T. K. Achar, R. Mondal, M. S. Shanavas, S. Maity, N. Pal and Prof. Dr. D. Maiti
Department of Chemistry
Indian Institute of Technology Bombay
Powai, Mumbai 400076, India
E-mail: dmaiti@chem.iitb.ac.in
[b] X. Zhang and Prof. Dr. R. S. Paton
Chemistry Research Laboratory, University of Oxford
Mansfield Road, Oxford OX1 3TA, United Kingdom
E-mail: robert.paton@colostate.edu

Supporting information for this article is given via a link at the end of the document.

Direct C–H allylation is an important method in view of atom and/or step economy and synthetic utility. In recent years, the synthetic community has witnessed a tremendous growth in *ortho*-C–H allylation reactions (Figure 1b).[8] To the best of our knowledge, distal *meta*-C–H allylation has not yet been reported. The allylation of aromatic compounds is an important transformation in organic synthesis as the allyl group offers a wealth of opportunities to access other functional groups.[9] Conventionally, aryl metal compounds like magnesium, zinc, and boron reagents have been utilized for transition metal catalyzed allylation with allylic electrophiles.[10] Despite excellent site-selectivity, these protocols suffer from unavoidable preactivation of arenes, thus requiring a stoichiometric amount of metals for metalation (Figure 1a). Later on, more straightforward approaches such as Lewis acid-promoted Friedel-Crafts allylation and Pd-catalyzed Tsuji-Trost reaction have been developed.[11] Numerous examples of transition metal catalyzed directed *ortho*-C–H allylation reactions have also been developed utilizing activated or prefunctionalized coupling partners, such as allyl halides, acetates, phosphates and carbonates (Figure 1b).[8a]

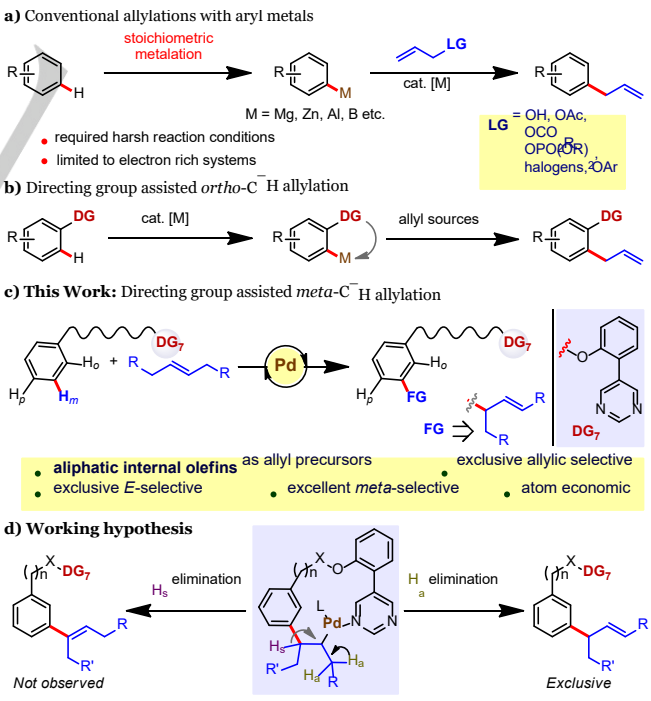


**Figure 1. C–H allylation reaction. a**, Traditional allylation with organometallic compounds with allylic electrophiles. **b**, Transition metal catalyzed directed *ortho*-C–H allylation. **c**, Palladium catalyzed *meta*-C–H allylation of arenes with unactivated internal olefins (this work). **d**, Working hypothesis.

Very few reports on utilizing unactivated allylic coupling partners have been reported in the literature.[8c, 12] Compared to the extensive studies on C–H alkenylation reactions with activated olefins, unactivated olefins have not been extensively employed in alkenylation reactions, presumably because of their inertness to undergo migratory insertion.[3d, 13] Recently, we have demonstrated the utilization of unactivated olefins for dehydrogenative heck reactions at the *ortho*-position with Pd and high-valent Co-catalyst.[3d, 8c, 12a] As part of our continuous effort to reach out to the distal *meta*-C–H bond, we envisioned a Pd-catalyzed *meta*-C–H allylation of arenes utilizing readily available unactivated internal olefins as allyl surrogates (Figure 1c). Upon 1,2-migratory insertion of olefins at the *meta*-position, the carbometallated intermediate opens up two different avenues which might lead to intricate mixtures of styrenyl and allylic products (Figure 1d). Utilization of the appropriate metal-ligand system favours formation of the allyl product over the thermodynamically more stable styrenyl product through conformational control exerted by the metallacycle. It is noteworthy that our method proceeds proficiently and provides exclusive *E*-selective allyl isomers in the presence of a catalytic amount of $Pd(OAc)_2$ and mono-protected amino acid (MPAA), *N*-acetyl norleucine ligand.

## Results and Discussion

**Evaluation of directing groups.** We initiated our investigation of *meta*-C–H allylation of arenes using a 3-methylbezylsulfonyl ester linked with different *meta*-directing groups (DGs) as a model substrate. Interestingly, it was found that the strongly coordinating pyrimidine based biphenyl DG (**$DG_7$**) was superior over others in terms of both yield and selectivity (Table 1). This can be attributed to strong σ-donating and π-accepting ability of the pyrimidine ring, which binds with the Pd-catalyst effectively and facilitates olefin coordination as well as migratory insertion.[14] Although **$DG_8$** is a strong σ-donor, its lower efficiency could be attributed to its bulkier size, which impedes olefin coordination as well as insertion. Under optimized conditions, exclusive allyl selective alkenylated products were achieved in synthetically useful yields.[15] Mono-protected amino acid (MPAA) ligand, *N*-acetyl norleucine, was found to be best for this particular transformation. Contrary to our previous studies, a nonpolar aprotic solvent, acetonitrile, considerably increased the efficiency of the protocol. We hypothesized that an apolar transition state of migratory insertion could be overall turnover-limiting, the stabilisation of which by the nonpolar solvent gives high yields. Gratifyingly, exclusive allyl product was achieved under aerobic conditions, instead of the Heck type styrenyl product.

**Scope of *meta*-selective C–H allylation.** The scope of this method was subsequently examined under optimal conditions. First, we evaluated several unactivated internal olefins (Figure 2a). Expectedly, higher homologue *trans*-5-decene and *trans*-7-tetradecene produced **3b** and **3c** with excellent yields.

**Table 1.** Evaluation of Directing Groups

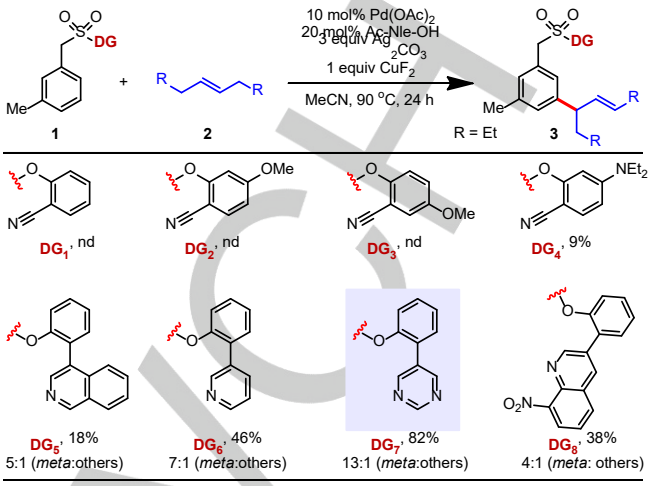


Presumably due to high volatility of *trans*-3-hexene, yield of **3d** was relatively lesser (66%). Next we turned our focus on functionalized internal olefins to evaluate the feasibility of the method. With different ester-based internal olefins, compounds **3h-n** were isolated in very good to excellent yields. *Trans*-2-octene and *trans*-3-octene provided the allyl products **3e** and **3f** with excellent regioisomeric ratios. With 4-methyl-2-pentene 2g, pharmaceutically relevant isoprenyl-type functionality was obtained in very good yield and selectivity (**3g**, 71%). Different natural products and drugs functionalized with unbiased internal olefins (**2j-n**) were found to be well tolerated under the optimized conditions.

Figure 2b demonstrated the generality of the allylation reaction with substituted benzylsulfonyl ester (**3o-z**) using *trans*-4-octene as an allyl surrogate. The reaction proceeded with a variety of electron-rich and electron-deficient sulfonyl ester containing functional groups such as Me, Br, F, Cl, $CF_3$, $OCF_3$. Interestingly, bromo-substituents turned out to be well tolerated without providing undesired side products under Pd-catalysis.

Following the successful implementation of *meta*-selective C–H allylation in benzylsulfonyl esters, several other scaffolds with linker variations such as phenethyl ether (**4**, Figure 3a), phenylacetic acid (**6**, Figure 3c) and benzylsillane (**8**, Figure 3d) were evaluated. In all cases, excellent yields and selectivities were observed irrespective of their electronic and steric nature. We examined the possibility of implementing the present protocol in late-stage C–H functionalization of drug molecules. Strikingly, phenylacetic acid based pharmaceuticals (**7b-d**) were shown to be compatible and provided good-to-excellent yields with very good selectivity. Similarly, internal olefins derived from naturally occurring oleic acid (**2i**), nerol (**2j**), cholesterol (**2l**), menthol (**2h**), adamantane (**2k**); drugs such as ibuprofen (**2m**), myristic acid (**2n**) were also well tolerated and showed comparable reactivity pattern.

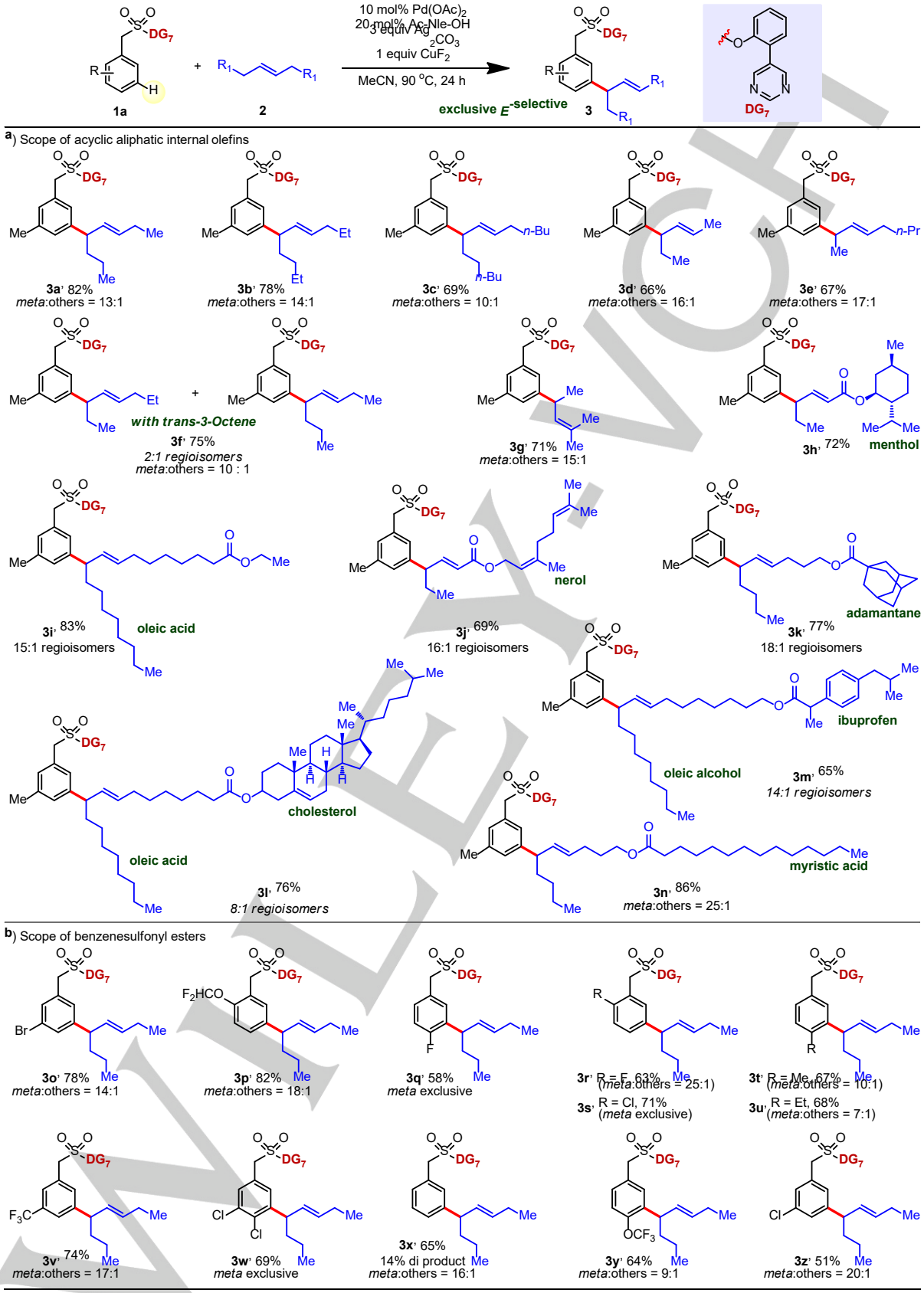


**Figure 2. Scope of the reaction. a**, Evaluation of the unactivated internal olefins with **1a**. **b**, Scope of the sulfonyl esters with **2a.**

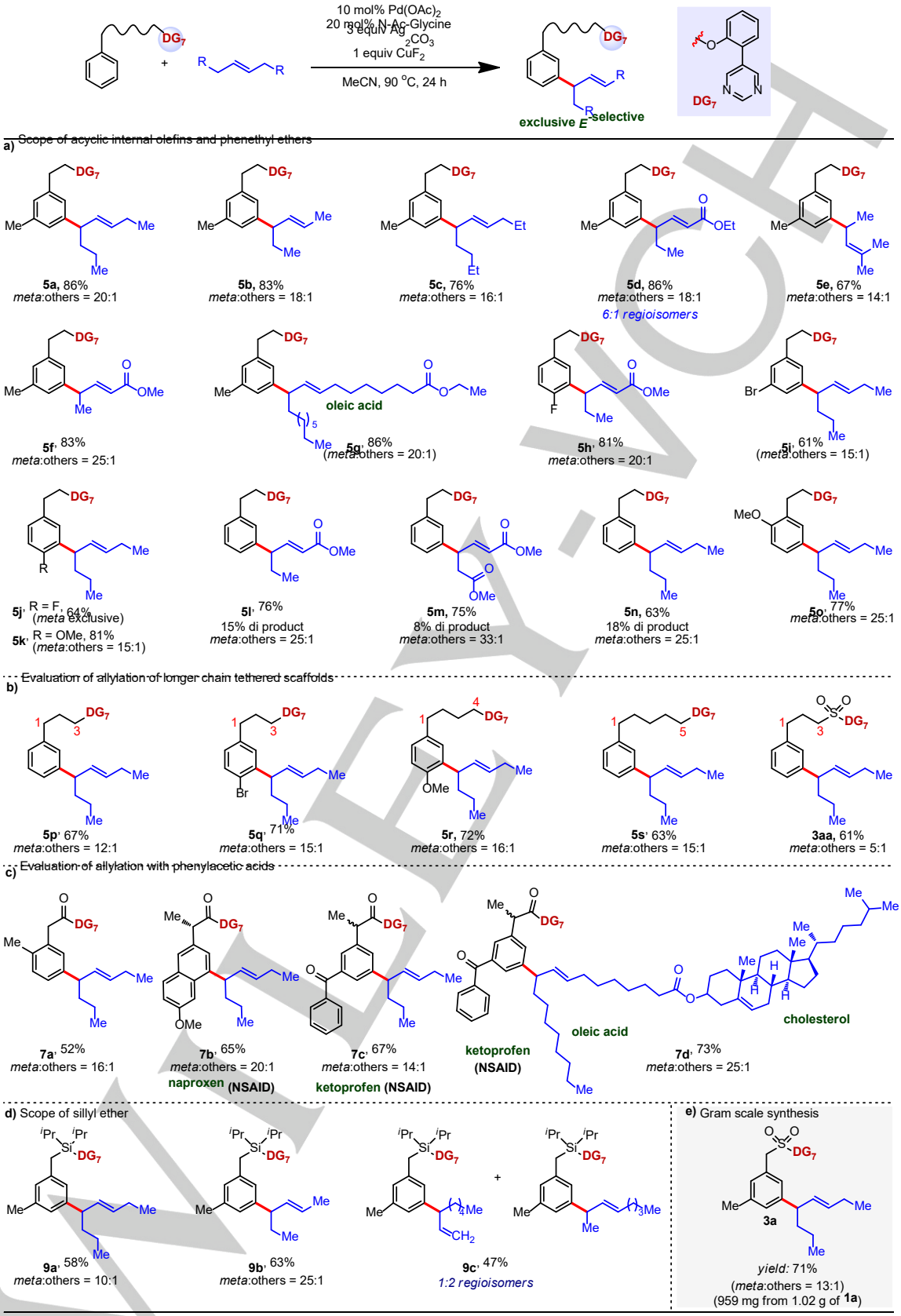


**Figure 3. *Meta*-selective C–H allylation. a**, Evaluation of *meta*-selective C–H allylation of phenethylethers. **b**, Allylation of longer chain tethered scaffolds. **c**, C–H allylation of phenylacetic acids. **d**, C–H allylation of silyl ethers. **e**, Gram-scale synthesis.

The generality, regioselectivity and stereoselectivity of this protocol were further investigated with substrates having an elongated template backbone (Figure 3b). In all cases, the desired *meta*-allyl products were afforded in synthetically useful yields and selectivity. To check the feasibility of the protocol in large scale, this reaction was scaled up to 3 mmol with substrate **1a** using a standard Schlenk flask, the desired allylated product was obtained in 71% yield with excellent selectivity (Figure 3e).

**Mechanistic investigation.** Experiments were carried out to elucidate the mechanism for this *meta*-selective C–H allylation reaction. Qualitative $^1$H NMR experiments revealed the indispensable role of Pd and ligand in this transformation (Supporting information (SI), 2.6.1).[15] In the presence of $Pd(OAc)_2$ and Ac-Nle-OH, a prominent chemical shift of **1a** suggested strong interactions with the catalyst and ligand (see SI, highlighted in colour shade), likely through the pyrimidine-N, which was further confirmed by the X-ray crystal structure (SI, 2.6.4). Kinetic studies suggested that the reaction rates of acyclic olefins (*cis*- and *trans*-olefins) are comparable and much higher (~ 4.8 times) than that of cyclic olefin (see SI, Figure S5). This was attributed to the free rotation along the C–C bond in the insertion intermediate (Figure 4, **int-4**) for both the *trans*- and *cis*-olefins, whereas this degree of rotational freedom for cyclic olefins was unlikely (see computational studies, Figure 7). Each reaction component was additionally shown to have crucial influences on the rate enhancement (see SI, Figure S6). A product distribution value of [$P_H/P_D$] = 1.08 was obtained from the competition experiment.[15] Kinetic isotope effect (KIE) studies revealed a $k_H/k_D$ value of 1.18, suggesting that the C–H activation step is unlikely the rate determining step (r.d.s.) of the overall transformation.[15]

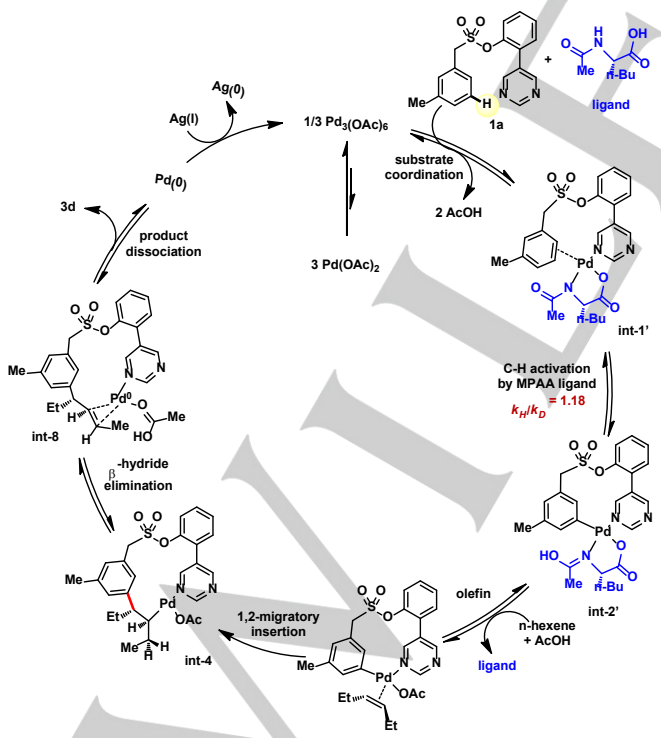


**Figure 4.** Catalytic cycle based on experimental mechanistic and computational studies.

**Computational Studies.** Density functional theory (DFT) calculations were performed using *Gaussian 16* software[16] to understand our Pd(II)-catalyzed template-assisted *meta*-selective C($sp^2$)–H allylation. Arene **1a** and *trans*-3-hexene were used in computations. Geometry optimizations were performed at MN15[17]/GENECP level of theory. This functional was chosen as it performs much better than many other functionals in predicting transition metal reaction barrier heights[17] and gives good experimental agreements in similar palladium catalysis studies.[18] The effects of acetonitrile solvent on the computed Gibbs energy profile were included by further single-point calculations (see SI 2.7 for full computational details). The overall Gibbs energy profile for the proposed catalytic cycle is shown in Figure 5. The reaction proceeded with C–H activation, followed by 1,2-migratory insertion of alkene and the subsequent $\beta$-hydride elimination to yield the final product (Figure 4a). In the absence of ligand, C–H activation (**ts-1**) was the turnover frequency-determining transition state (TDTS)[19] and unfavourable. The coordination of amino acid ligand, Ac-Nle-OH, with displacement of *two* acetic acid molecules, was entropically favoured. Transition structure **ts-1'** has the characteristic [5,6]-palladacycle conducive for C–H activation.[6b, 20] The formation of a 5-membered palladacycle by the ligand strategically positions the amide oxygen for facile C–H activation *via* concerted metalation deprotonation (CMD) (other possible ligand arrangements were not competitive, see SI 2.7.2). With the ligand lowering C–H activation, 1,2-migratory insertion became the overall TDTS with an activation barrier of 24.3 kcal mol$^{-1}$. This is consistent with our experimental studies: the computed reaction coordinate predicts a reaction first order in alkene, a reversible C–H activation step, and an absence of a primary C–H KIE. The secondary C–H KIE results from the insertion step. For modelling purposes and simplicity, we replaced the amino acid ligand by acetate in subsequent steps, as both the ligand and acetate act in a monodentate fashion and the Pd–N coordination interactions would dominate over any additional non-covalent interactions (NCIs) that the amino acid side chain would have (see SI 2.7.3 for a complete discussion). Although the overall TDTS of the reaction was 1,2-migratory insertion (see SI 2.7.6 for arene site selectivity studies), the regio-(allyl/styrenyl) and stereo-(*E/Z*) selectivities are determined by the subsequent $\beta$-hydride elimination step. Direct $\beta$-hydride elimination required positioning the ligand in close proximity with the palladacycle ring, giving unfavourable sterics in **int-5**, which subsequently proceeded *via* **ts-5** to give the desired product. This left palladium in +2 oxidation state forming metal-bonded hydride **int-6** that could further undergo reductive elimination to generate Pd(0) catalyst. More favourably, a facile rotation in C–C bond (**ts-6**)

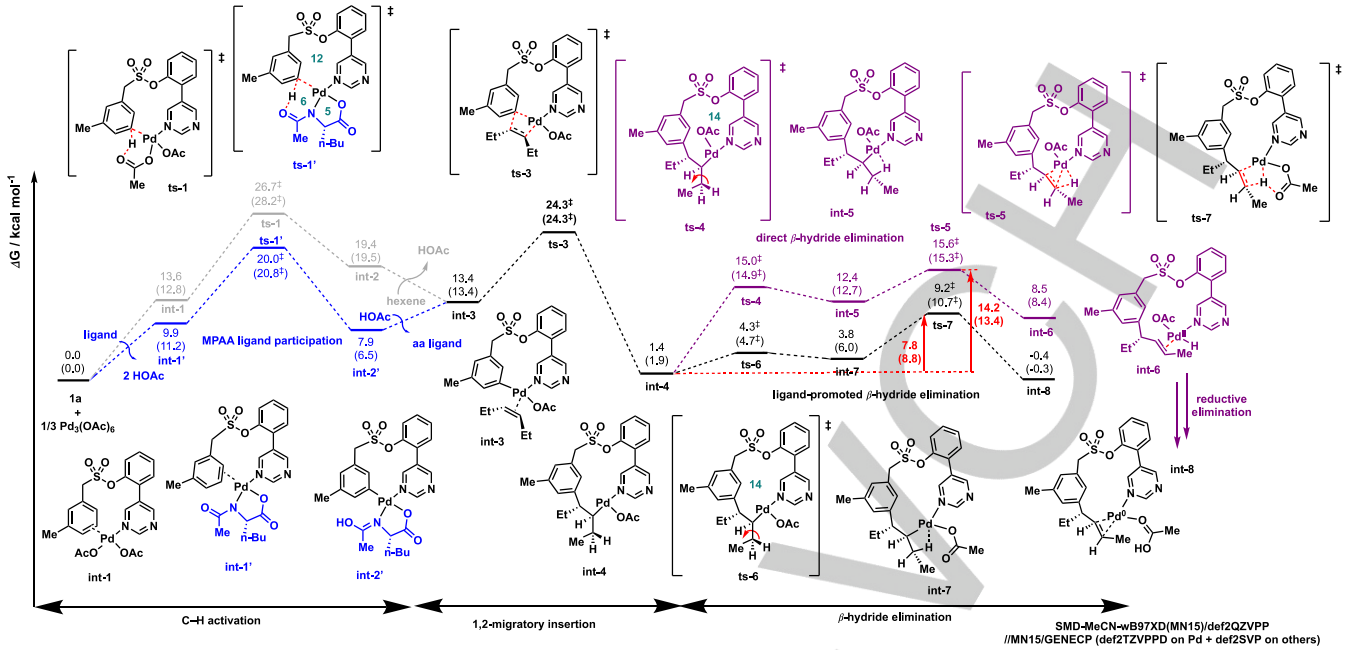


**Figure 5.** Computed Gibbs energy profile.

strategically positioned the acetate for ligand-assisted *β*-hydride elimination (**ts-7**), giving final product **int-8** directly and regenerating Pd(0) (**int-7** is lower in energy than **int-5** due to more favourable sterics, see SI 2.7.4). This product **int-8** was exergonic and irreversible, such that **ts-7** is overall stereo-determining.

To understand the regio- (allyl/styrenyl) as well as stereo- (*E*/*Z*-selectivity for the allyl product) selectivity in product formation, we performed a detailed study of the *β*-hydride elimination step (SI section 2.7.5). Allylation proceeded *via* ligand-promoted *β*-H elimination whereas styrenylation direct *β*-H elimination *via* a Pd(II)-hydride complex. The formation of *Z*-allylated product had a barrier that was 2.1 kcal mol$^{-1}$ higher than *E*-allylated product, thus being disfavoured (1 in 18). Their HOMOs are almost identical, showing similar electron movements in the TSs; NCI plots shows that *Z*-allylation was disfavoured due to unfavourable 1,3-diaxial interactions arising from the arrangement of the methyl side group (Figure 6). Styrenylation (ts-5b) had a barrier that is 17.8 kcal mol$^{-1}$ higher than *E*-allylation (ts-7), making styrenylation impossible (1 in 50 billion). It is difficult to see, from the HOMOs and NCI plots how ts-5b was hugely disfavoured compared to allylation TSs. However, we note that the rotational barrier ts-4b for styrenyl-product formation was very close to ts-5b (within 1 kcal mol$^{-1}$) and it was hugely disfavoured since rotating the C–C bond to bring the hydrogen atom $H_S$ in position to interact agostically with Pd(II) centre introduced a massive strain in the 14-membered palladacycle, evidenced by the geometry changes when $H_S$ came close to Pd(II) centre (Figure S16 (ii)). It is worth noting that the regioselectivities were not controlled by orbital interactions but rather by the conformational restraints due to the conformationally rigid 14-membered palladacycle. This is evident since allylation did not involve the distortion of 14-membered palladacycle (the ligand-promoted *β*-H elimination occurred outside the palladacycle without distorting it) whereas styrenylation required first bringing $H_S$ (on the carbon atom forming part of the palladacycle, Fig. 6b) to interact with Pd(II)-centre agostically before subsequent *β*-H elimination, thus introducing unfavourable ring strains in the 14-membered palladacycle.

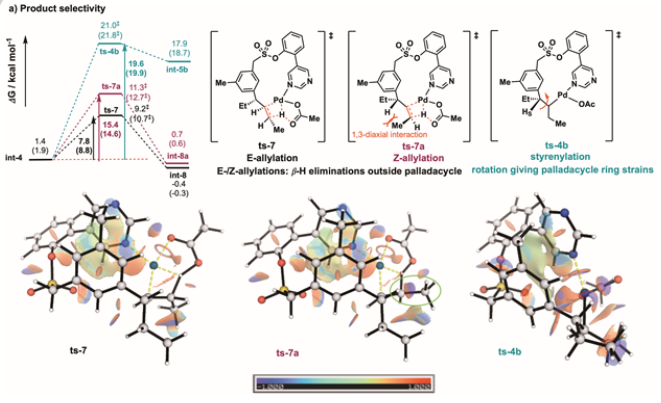


**Figure 6.** Product selectivity studies comparing E-/Z-allyl- vs styrenyl-product formations for *trans*-hexene substrate.

Experimentally, *cis*-olefin was found to be slightly less reactive than *trans*-olefin, we modelled the TDTS (1,2-migratory insertion) of *cis*-olefin and compared this to *trans*-olefin. Since there were numerous conformers close in energy (within 5 kcal

mol$^{-1}$), conformational samplings of the TDTSs for *cis*-olefins were again performed and Boltzmann weighted for comparison (SI 2.7.8). We can do this comparison since the reaction mechanism is the same for both olefin substrates and the lowest resting states were the separated reactants (see SI for details on conformational sampling of the TDTSs). A ratio of 1.2 : 1 (*trans*-hexene vs *cis*-hexene) for the relative rates were obtained using $\omega$B97X-D functional for SP correction whereas this ratio reversed and became 1 : 1.3 using MN15 functional. This suggests that the reactivity for either olefin would be comparable, mirroring the experimental observation (Figure S5). The product selectivities for *cis*-hexene were similarly studied (SI 2.7.9). As before, *E*-allylation (***cis*-ts-7**) had the lowest barrier, at 13.8 kcal mol$^{-1}$. The barrier for *Z*-allylation (***cis*-ts-7a**) was 3.6 kcal mol$^{-1}$ higher (1 in 147) and can be traced to the steric clashes (less favourable 1,3-diaxial interactions in *Z*-allylation) as evidenced by the NCI plots (Figure S22). Styrenylation was once again uncompetitive, as for *trans*-hexene, due to the unfavourable ring strains experienced by the palladacycle when the styrenyl proton $H_S$ was brought to interact agostically with Pd(II)-centre (Figure S23ii). It is important to realise that allylation has $\beta$-H elimination occurring outside the rigid palladacyle insertion intermediate whereas styrenylation has $\beta$-H elimination incurring unfavourable distortions of the palladacyle (Figure 7(i)).

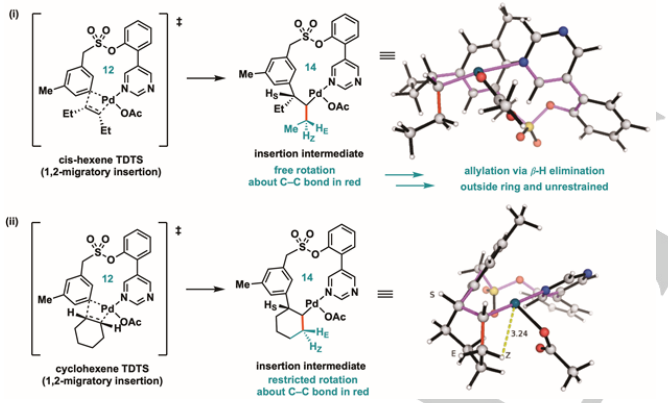


**Figure 7.** (i) Free C–C rotations in *cis*-hexene without imposing ring strain. (ii) Restricted C–C rotations in cyclohexene giving rise to unduly strained palladacycle.

Cyclohexene was next compared to *trans*-olefin in terms of the energetics of the 1,2-migratory insertion TDTS. Boltzmann weighting of the conformers gave a ratio of 1:44–56 (cyclohexene vs *trans*-hexene) for relative rates. This is in agreement with experimental observation that the reaction with cyclooctene proceeded significantly slower than that with *trans*-hexene (Figure S5). The product selectivities for cyclohexene substrate were studied (SI 2.7.10) and it was found that only *Z*-allylation could be possible (Fig. S24), with a barrier of 17.3 kcal mol$^{-1}$ (**cy-ts-7a**, Figure S25). The cyclohexene ring severely restricts the degree of rotational freedom in the intermediate after insertion: both the $H_E$ and $H_S$ atom could not be brought to interact agostically with Pd(II) centre without incurring unduly strains due to geometric constraints placed by the cyclohexene ring (Figure 7(ii)). Thus, if at all, the allylation product would adopt *Z*-geometry that formed part of the cyclohexene ring. The *Z*-allylated product **cy-int-8a** is endergonic with respect to the insertion intermediate **cy-int-4**, making this product formation thermodynamically reversible, thus explaining its poor yield obtained experimentally.

Based on our experimental and computational mechanistic studies, we propose a catalytic cycle for the *meta*-selective C–H allylation reaction (Figure 4). We believe that arene **1a** coordinates to the palladium catalyst and subsequently, MPAA-assisted *meta*-hydrogen abstraction from the arene leads to C–H activated intermediate **int-2'**. Coordination of electronically unbiased internal olefins and the subsequent rate-determining migratory insertion afford a cyclophane-like 14-membered metallacycle **int-4** which further undergoes selective $\beta$-H elimination to deliver **3d**. Stability and conformational restraints of intermediate **int-4** play a crucial role for both regio- and stereo-selective outcomes of this reaction: the rotational TSs for allylation and the subsequent ligand-assisted $\beta$-H elimination occur outside the conformationally rigid metallacycle whereas the rotational TS for styrenylation incurs huge ring strains in the metallacycle which has to be twisted in order to bring the requisite H atom to interact with Pd(II)-centre agostically before subsequent $\beta$-H elimination could occur.

## Conclusion

In summary, we have presented an unprecedented approach to distal *meta*-selective C–H allylation using unactivated internal olefins as allyl surrogates. This operationally simple, atom-economical and catalytically efficient approach demonstrates impressive functional group tolerance, substrate scopes and product yields. Additionally, remarkable late-stage functionalisations of drug molecules are achieved. Computations provide us an augmented understanding of the reaction mechanism: 1,2-migratory insertion is the overall turnover frequency-determining transition state whereas selective $\beta$-H elimination determines the product identity. The product selectivities are dictated by the sterics imposed by the substrate and the conformational rigidity afforded by the palladacycle intermediate in the $\beta$-H elimination step. We believe that these findings will stimulate further research on the utilization of unactivated internal olefins as powerful coupling partners.

## Experimental Section

**General procedure for palladium catalyzed *meta*-selective C□H allylation of arene.** To an oven-dried screw cap reaction tube charged with a magnetic stir-bar was added sulfonate ester/ether scaffold (0.2 mmol, 1 equiv), $Pd(OAc)_2$ (10 mol%), *N*-acetylnorleucine (20 mol%), $Ag_2CO_3$ (3 equiv) and $CuF_2$ (1 equiv). Aliphatic internal olefins (2 equiv) was added with a micro litter pipette and 2 mL acetonitrile was added with a disposable laboratory syringe under aerobic condition. The tube was

placed in a preheated oil bath at 90 ºC and the reaction mixture was stirred for 24 h. The reaction mixture was then cooled to room temperature and filtered through a celite pad with ethyl acetate. The filtrate was concentrated and the crude compound was purified by column chromatography using silica gel (100-200 mesh size) and petroleum ether / ethyl acetate as an eluent.

## Acknowledgements

We are thankful to SERB-India (CRG/2018/003951), SERB-NPDF (TKA; PDF/2016/002187) for financial support. Funding from A*STAR Singapore (X.Z.) is gratefully acknowledged. X.Z. and R.S.P. acknowledge the EPSRC Centre for Doctoral Training in Theory and Modelling in Chemical Sciences (EP/L015722/1) and the use of Dirac cluster at Oxford.

**Keywords:** keyword 1 • keyword 2 • keyword 3 • keyword 4 • keyword 5

[1] a) J. Yamaguchi, A. D. Yamaguchi, K. Itami, *Angew. Chem. Int. Ed.* **2012**, *51*, 8960-9009; b)J. Wencel-Delord, F. Glorius, *Nat. Chem.* **2013**, *5*, 369.

[2] a)S. R. Neufeldt, M. S. Sanford, *Acc. Chem. Res.* **2012**, *45*, 936-946; b)M. Tobisu, N. Chatani, *Science* **2014**, *343*, 850-851; c)K. M. Engle, T.-S. Mei, M. Wasa, J.-Q. Yu, *Acc. Chem. Res.* **2012**, *45*, 788-802.

[3] a)L. Ackermann, R. Vicente, A. R. Kapdi, *Angew. Chem. Int. Ed.* **2009**, *48*, 9792-9826; b)H. P. L. Gemoets, I. Kalvet, A. V. Nyuchev, N. Erdmann, V. Hessel, F. Schoenebeck, T. Noel, *Chem. Sci.* **2017**, *8*, 1046-1055; c)M. S. Sigman, E. W. Werner, *Acc. Chem. Res.* **2012**, *45*, 874-884; d)A. Deb, S. Bag, R. Kancherla, D. Maiti, *J. Am. Chem. Soc.* **2014**, *136*, 13602-13605.

[4] a)R.-Y. Tang, G. Li, J.-Q. Yu, *Nature* **2014**, *507*, 215-220; b)H. J. Davis, M. T. Mihai, R. J. Phipps, *J. Am. Chem. Soc.* **2016**, *138*, 12759-12762; c)Z. Ruan, S.-K. Zhang, C. Zhu, P. N. Ruth, D. Stalke, L. Ackermann, *Angew. Chem. Int. Ed.* **2017**, *56*, 2045-2049; d)Z. Dong, J. Wang, G. Dong, *J. Am. Chem. Soc.* **2015**, *137*, 5887-5890; e)O. Saidi, J. Marafie, A. E. W. Ledger, P. M. Liu, M. F. Mahon, G. Kociok-Köhn, M. K. Whittlesey, C. G. Frost, *J. Am. Chem. Soc.* **2011**, *133*, 19298-19301; f)S. Bag, T. Patra, A. Modak, A. Deb, S. Maity, U. Dutta, A. Dey, R. Kancherla, A. Maji, A. Hazra, M. Bera, D. Maiti, *J. Am. Chem. Soc.* **2015**, *137*, 11888-11891.

[5] a)D. Leow, G. Li, T.-S. Mei, J.-Q. Yu, *Nature* **2012**, *486*, 518; b)S. Lee, H. Lee, K. L. Tan, *J. Am. Chem. Soc.* **2013**, *135*, 18778-18781; c)M. Bera, A. Maji, S. K. Sahoo, D. Maiti, *Angew. Chem. Int. Ed.* **2015**, *54*, 8515-8519; d)S. Li, H. Ji, L. Cai, G. Li, *Chem. Sci.* **2015**, *6*, 5595-5600; e)A. Dey, S. K. Sinha, T. K. Achar, D. Maiti, *Angew. Chem. Int. Ed.*, *doi:10.1002/anie.201812116*, doi:10.1002/anie.201812116.

[6] a)R. Jayarajan, J. Das, S. Bag, R. Chowdhury, D. Maiti, *Angew. Chem. Int. Ed.* **2018**, *57*, 7659-7663; b)U. Dutta, A. Modak, B. Bhaskararao, M. Bera, S. Bag, A. Mondal, D. W. Lupton, R. B. Sunoj, D. Maiti, *ACS Catal.* **2017**, *7*, 3162-3168; c)A. Maji, A. Dahiya, G. Lu, T. Bhattacharya, M. Brochetta, G. Zanoni, P. Liu, D. Maiti, *Nat. Commun.* **2018**, *9*, 3582.

[7] a)S. Bag, R. Jayarajan, R. Mondal, D. Maiti, *Angew. Chem. Int. Ed.* **2017**, *56*, 3182-3186; b)S. Bag, R. Jayarajan, U. Dutta, R. Chowdhury, R. Mondal, D. Maiti, *Angew. Chem. Int. Ed.* **2017**, *56*, 12538-12542.

[8] a)N. K. Mishra, S. Sharma, J. Park, S. Han, I. S. Kim, *ACS Catal.* **2017**, *7*, 2821-2847; b)H. Wang, N. Schröder, F. Glorius, *Angew. Chem. Int. Ed.* **2013**, *52*, 5386-5389; c)S. Maity, P. Dolui, R. Kancherla, D. Maiti, *Chem. Sci.* **2017**, *8*, 5181-5185.

[9] a)B. M. Trost, F. D. Toste, *J. Am. Chem. Soc.* **2000**, *122*, 11262-11263; b)B. M. Trost, O. R. Thiel, H.-C. Tsui, *J. Am. Chem. Soc.* **2002**, *124*, 11616-11617.

[10] a)P. A. Evans, D. Uraguchi, *J. Am. Chem. Soc.* **2003**, *125*, 7158-7159; b)M. A. Kacprzynski, T. L. May, S. A. Kazane, A. H. Hoveyda, *Angew. Chem. Int. Ed.* **2007**, *46*, 4554-4558; c)Y. Kiyotsuka, H. P. Acharya, Y. Katayama, T. Hyodo, Y. Kobayashi, *Org. Lett.* **2008**, *10*, 1719-1722; d)N. Harrington-Frost, H. Leuser, M. I. Calaza, F. F. Kneisel, P. Knochel, *Org. Lett.* **2003**, *5*, 2111-2114.

[11] a)M. Niggemann, M. J. Meel, *Angew. Chem. Int. Ed.* **2010**, *49*, 3684-3687; b)J. Tsuji, *Tetrahedron* **1986**, *42*, 4361-4401; c)B. M. Trost, M. L. Crawley, *Chem. Rev.* **2003**, *103*, 2921-2944.

[12] a)S. Maity, R. Kancherla, U. Dhawa, E. Hoque, S. Pimparkar, D. Maiti, *ACS Catal.* **2016**, *6*, 5493-5499; b)T. Yamaguchi, Y. Kommagalla, Y. Aihara, N. Chatani, *Chem. Commun.* **2016**, *52*, 10129-10132.

[13] P. Basnet, S. Kc, R. K. Dhungana, B. Shrestha, T. J. Boyle, R. Giri, *J. Am. Chem. Soc.* **2018**, *140* 15586–15590.

[14] "s-Pyridine Coordination Compounds with Transition Metals": Chemistry of Heterocyclic Compounds: Pyridine Metal Complexes, Part 6, Vol. 14, (Eds.: P. Tomasik, Z. Rataje-wicz, G. R. Newkome, L. Strekowski), Wiley, Hoboken, Ch. 3,1985; "p-Coordination Compounds of Pyridines with Metals": Chemistry of Heterocyclic Compounds: Pyridine Metal Complexes, Part 6, Vol. 14 (Eds.: P. Tomasik, Z. Rataje-wicz, G. R. Newkome, L. Strekowski), Wiley, Hoboken, 1985, Ch. 5.

[15] For detailed studies, see the Supporting Information File

[16] Frisch, M. J. et al. Gaussian 16, Revision A.01. (2016).

[17] H. S. Yu, X. He, S. L. Li, D. G. Truhlar, *Chem. Sci.* **2016**, *7*, 5032-5051.

[18] S. Guin, P. Dolui, X. Zhang, S. Paul, V. K. Singh, S. Pradhan, H. B. Chandrashekar, S. S. Anjana, R. S. Paton, D. Maiti, *Angew. Chem. Int. Ed.*, *0*, 10.1002/anie.201900479.

[19] S. Kozuch, S. Shaik, *Acc. Chem. Res.* **2011**, *44*, 101-110.

[20] a)G. Chen, W. Gong, Z. Zhuang, M. S. Andrä, Y.-Q. Chen, X. Hong, Y.-F. Yang, T. Liu, K. N. Houk, J.-Q. Yu, *Science* **2016**, *353*, 1023; b)G.-J. Cheng, Y.-F. Yang, P. Liu, P. Chen, T.-Y. Sun, G. Li, X. Zhang, K. N. Houk, J.-Q. Yu, Y.-D. Wu, *J. Am. Chem. Soc.* **2014**, *136*, 894-897; c)Y.-F. Yang, X. Hong, J.-Q. Yu, K. N. Houk, *Acc. Chem. Res.* **2017**, *50*, 2853-2860.

**Entry for the Table of Contents**

Layout 2:

RESEARCH ARTICLE

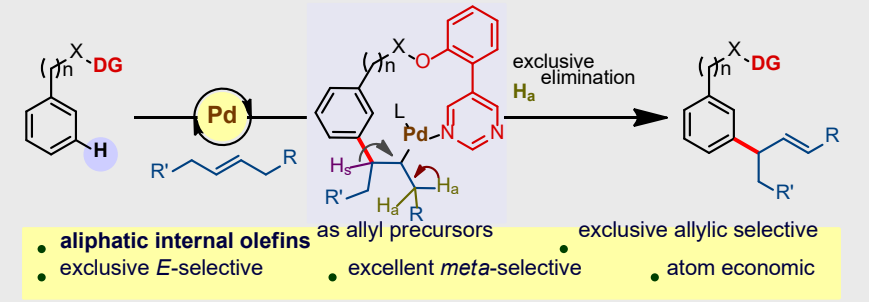


Palladium(II)-catalyzed *meta*-selective C–H allylation of arenes has been developed utilizing synthetically inert unbiased acyclic aliphatic olefins as allylic surrogates.

*Tapas Kumar Achar,[§,†] Xinglong Zhang,[§,‡] Rahul Mondal,[†] M. S. Shanavas,[†] Sabyasachi Maity,[†] Nityananda Pal,[†] Robert S. Paton,*[‡] and Debabrata Maiti*[†]*

***Page No. – Page No.***

**Palladium-Catalyzed Directed *meta*-Selective C–H Allylation of Arenes: Unactivated Internal Olefins as Allyl Surrogates**